Conformations of Diethoxymethane: Matrix Isolation Infrared and ab Initio Studies

V. Venkatesan, K. Sundararajan, and K. S. Viswanathan*

Materials Chemistry Division, Indira Gandhi Centre for Atomic Research, Kalpakkam 603 102 India

Received: May 6, 2003; In Final Form: July 7, 2003

Conformations of diethoxymethane (DEM) were studied using matrix isolation infrared spectroscopy. DEM was trapped in an argon matrix using an effusive source maintained at various temperatures: 298, 388, and 430 K. The elevated temperatures were used to increase the population of the higher energy conformers in the matrix. As a result of these experiments, infrared spectra of the ground, $\mathbf{G^{\pm}G^{\mp}(tt)}$, and higher energy conformers, $\mathbf{G^{+}G^{-}(g^{+}t)}$, $\mathbf{G^{+}G^{-}(g^{-}t)}$, and $\mathbf{TG^{\pm}(tt)}$, of DEM are reported, for the first time. The experimental studies were supported by ab initio computations performed at B3LYP level, using a 6-31++G** basis set.

Introduction

The anomeric effect associated with the COCOC framework directs the molecule to adopt a gauche orientation rather than trans, thereby enabling the delocalization of the oxygen lone pair into a low-lying antiadjacent σ^*_{c-o} orbital.[1,2] However, the anomeric stabilization may be opposed or enhanced by the other interactions, chief among them being steric. The interplay of these factors decides the relative stability of the different conformers in a molecule. These factors are expected to play an important role in determining the conformational stabilities of simple acyclic acetals and ketals. In dimethoxymethane (DMM), anomeric stabilization is the factor that significantly contributes toward conformational stability.[3,4] In substituted methoxymethanes, such as 1,1-dimethoxyethane (DME) and 2,2-dimethoxypropane (DMP), the methyl substituents on the central carbon atom increases the steric interactions along the central C−O bonds. Recently, we had published a detailed experimental and computational study on the conformers of DMM, DME, and DMP,[5−7] wherein we had presented infrared spectra for the ground state $\mathbf{G^{\pm}G^{\mp}}$ and the first higher energy **TG** conformers of DMM, DME, and DMP isolated in solid Ar and N_2 matrixes. These studies clearly showed the relative interplay between anomeric stabilization and steric interactions due to substitution on the central carbon atom in deciding the relative energies of the various conformers of these molecules.

In the present study, we have examined the effect of terminal substituents on the stability of the conformers of molecules such as diethoxymethane (DEM). With its longer alkyl chain, DEM can be expected to have a larger number of stable conformers and therefore present a more complex problem than DMM. Little is known on the conformations of DEM. Nukada[8,9] had assigned the vibrational features in DEM, though in his work that dealt with liquid and solid samples, the conformational aspects had not been discussed in any great detail. Experimental data was sparse for any definitive assignment to be made for the conformers of DEM. Furthermore, in the liquid and solid phases, the infrared spectral features of the different conformers were not resolved and unambiguous assignments were therefore not possible. Also, no computational work has been done on the structures and energies of DEM. We have therefore, for the first time, studied the conformers of DEM, using matrix isolation infrared spectroscopy and ab initio computations.

* Corresponding author. E-mail: vish@igcar.ernet.in.

Experimental Section

Matrix isolation experiments were performed using a Leybold AG closed cycle helium compressor cooled cryostat, RD210. The details of the vacuum and cryogenic systems have been discussed elsewhere.[10−12]

DEM (Merck, >99%) and the matrix gas argon (IOLAR Grade I) were first mixed to the desired ratio (DEM/Ar 1:1000) in a mixing chamber. This gas mixture was then deposited using an effusive source onto a KBr substrate maintained at 12 K. The deposition rate was typically ∼3 mmol h^{-1} and typical deposition times lasted ∼45 min. In an effort to increase the population of the higher energy conformers, we used elevated nozzle temperatures, 388 and 430 K, for some experiments. In the hot nozzle experiments, the nozzle was heated over a length of 35 mm to the required temperatures.

The IR spectra (4000−400 cm^{-1}) of the deposited species were recorded using a Bomem MB 100 FTIR spectrometer with spectral resolution of 1 cm^{-1}. The matrix was then warmed to 35 K, kept at this temperature for about 30 min, and then recooled to ∼12 K. The spectra of the matrix thus annealed were again recorded.

Computational Methods

Ab initio molecular orbital calculations were performed using the Gaussian 94W program[13] on an Intel Pentium II 233 MHz machine. Geometry optimizations were done at the B3LYP level with analytical gradients, using a 6-31++G** basis set, to obtain minima corresponding to the various conformers. All geometric parameters were allowed to be optimized, and no constraints were imposed on the molecular geometry during the optimization process.

Vibrational frequencies were calculated at the B3LYP/6-31++G** level using analytical derivatives. The B3LYP frequencies were used to compare our experimental frequencies with computations. It has been shown[5] that the frequencies computed at the B3LYP level provided a better agreement with the experimental frequencies and intensities of the features of DMM than did the HF computations. A similar trend was observed in the present study and hence only the B3LYP calculations have been shown. Zero-point energies (ZPE) obtained from the frequency calculations were used to calculate the ZPE corrected relative energies for the different conformers.

The computed frequencies of the various modes of the conformers of these molecules were used to simulate a

10.1021/jp035221g CCC: $25.00
Published on Web 09/09/2003

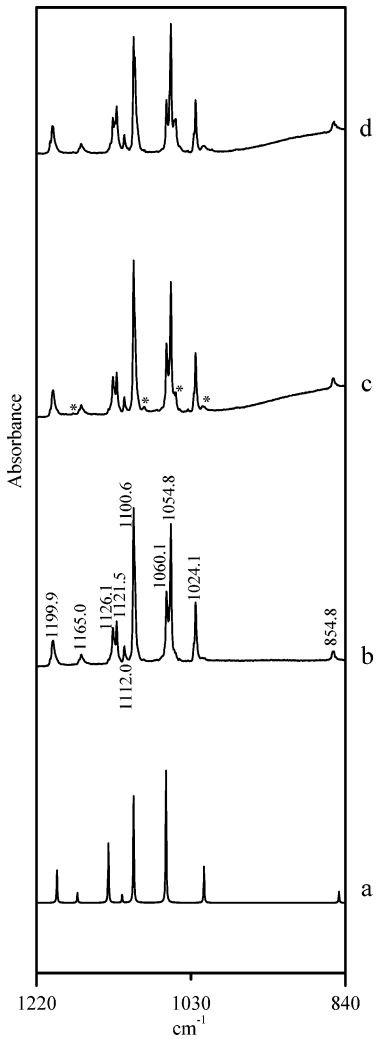

Figure 1. Computed and experimental spectra of DEM. (a) Computed spectrum for the ground-state $\mathbf{G^{\pm}G^{\mp}(tt)}$ conformer. Matrix-isolated DEM in preannealed Ar matrix (1:1000) using an effusive source with the nozzle temperature was maintained at (b) 298 and (c) 430 K. (d) Matrix deposited using a 430 K hot nozzle source annealed at 35 K.

vibrational spectra using SYNSPEC program.[14] For this exercise, the computed frequencies and the intensities at the B3LYP level were used and the spectra were constructed assuming a Lorentzian line profile with an fwhm of 1 cm^{-1}, which are typical line widths in our experiments.

Results

Experimental Results. Figure 1 shows the infrared spectra of DEM trapped in Ar, in the region of 840−1220 cm^{-1}, which corresponds to the C−O stretching, C−C stretching, CH_2 rocking, and CH_3 deformation vibrations. The DEM/Ar ratio was 1:1000 in all these experiments. When the temperature of the effusive source was maintained at 298 K, the main spectral features of matrix-isolated DEM occur at 854.8, 1024.1, 1054.8, 1060.1, 1100.6, 1112.0, 1121.5, 1126.1, 1165.0, and 1199.9 cm^{-1} (Figure 1b). When the matrix was annealed at 35 K, and the spectrum again recorded, no appreciable changes in the majority of spectral features were obtained.

Experiments were then performed using heated effusive nozzles, with the nozzle temperature maintained at 388 and 430 K. Figure 1c shows the spectrum obtained using the hot nozzle effusive source at 430 K. This spectrum corresponds to a preannealed matrix; the spectrum corresponding to the annealed matrix is shown in Figure 1d. It can be seen that certain features, indicated with asterisks, clearly appeared in this spectrum, most of which were barely observed in that obtained using a room-temperature effusive source (Figure 1b). Hence, these features may be expected to arise because of the higher energy conformers.

We have also examined spectra over the 1350 and 3000 cm^{-1} regions, which correspond to the CH_3 deformation and C−H stretching vibrations. However, the features in these regions could not be clearly resolved for the different conformations and hence are not shown nor discussed.

The normal mode descriptions in the acetals are quite complex because of the coupling of various C−O stretching and C−H deformation modes. Dasgupta et al.[15] have pointed out that contributions from the two types of force constants are almost about equal and the dominant character of any of the vibrations cannot be unambiguously assigned. We therefore made no attempt in this work to make a detailed assignment of the various frequencies.

All of the above experimental observations will now be discussed through a comparison with our computational results.

TABLE 1: Some Selected Important Structural Parameters[a] of the Various Conformers of DEM Computed at the B3LYP/6-31++G Level**

parameter	$G^{\pm}G^{\mp}(tt)$	$G^{+}G^{-}(g^{+}t)$	$G^{+}G^{-}(g^{-}t)$	$TG^{\pm}(tt)$	$G^{+}G^{-}(g^{+}g^{+})$
C^1-O^2	1.432	1.437	1.434	1.423	1.437
C^3-O^2	1.406	1.408	1.406	1.418	1.409
C^3-O^4	1.407	1.407	1.408	1.387	1.409
C^5-O^4	1.432	1.432	1.432	1.434	1.437
C^5-C^8	1.519	1.519	1.519	1.519	1.526
C^1-C^{11}	1.519	1.526	1.526	1.520	1.526
$O^4C^3O^2C^1$	69.5	71.6	74.2	180.5	69.9
$C^5\,O^4C^3O^2$	69.0	67.2	70.2	68.0	70.2
$C^8C^5O^4C^3$	176.6	175.8	175.8	173.6	87.1
$C^{11}C^1O^2C^3$	176.5	87.4	−92.6	180.3	87.3

parameter	$G^{+}G^{-}(g^{+}g^{-})$	$G^{+}G^{-}(g^{-}g^{-})$	$TG^{+}(tg^{-})$	$TG^{+}(g^{-}t)$	$TG^{+}(tg^{+})$
C^1-O^2	1.437	1.433	1.424	1.435	1.423
C^3-O^2	1.409	1.407	1.420	1.419	1.419
C^3-O^4	1.406	1.407	1.385	1.389	1.388
C^5-O^4	1.435	1.433	1.437	1.433	1.438
C^5-C^8	1.525	1.526	1.524	1.519	1.526
C^1-C^{11}	1.526	1.526	1.520	1.528	1.520
$O^4C^3O^2C^1$	72.3	81.6	179.6	198.4	182.8
$C^5\,O^4C^3O^2$	71.5	81.1	69.4	67.1	72.0
$C^8C^5O^4C^3$	−94.7	−83.5	−100.2	175.2	86.5
$C^{11}C^1O^2C^3$	87.0	−83.1	179.7	−73.7	180.0

parameter	$TG^{+}(g^{+}t)$	$TG^{+}(g^{-}g^{-})$	$TG^{+}(g^{-}g^{+})$	$TG^{+}(g^{+}g^{-})$	$TG^{+}(g^{+}g^{+})$
C^1-O^2	1.425	1.426	1.425	1.426	1.426
C^3-O^2	1.419	1.421	1.420	1.421	1.421
C^3-O^4	1.389	1.387	1.391	1.388	1.389
C^5-O^4	1.433	1.437	1.437	1.436	1.438
C^5-C^8	1.519	1.524	1.526	1.525	1.526
C^1-C^{11}	1.529	1.529	1.528	1.529	1.529
$O^4C^3O^2C^1$	160.5	193.2	197.7	159.7	169.0
$C^5\,O^4C^3O^2$	68.4	66.7	70.5	73.3	74.2
$C^8C^5O^4C^3$	173.9	−102.5	87.3	−94.4	88.3
$C^{11}C^1O^2C^3$	74.5	−74.7	−73.3	74.8	77.5

[a] Bond lengths in angstroms and bond angles and dihedral angles in degrees.

Computations

For the purposes of conformational studies, DEM can be considered as an extension of DMM (dimethoxymethane), with the alkyl group in DEM having one more carbon atom than in DMM. Consequently, the conformers for DEM may be viewed as correlating with those of DMM. Our earlier studies showed

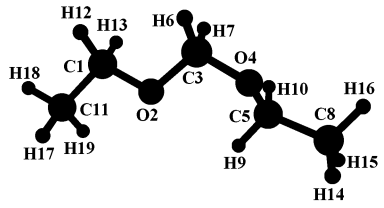

$TG^{\pm}$(tt) 2.15

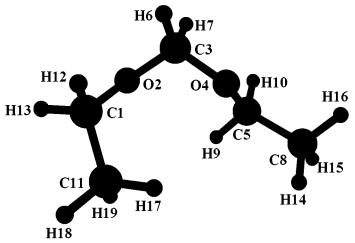

$G^{+}G^{-}(g^{-}t)$ 1.56

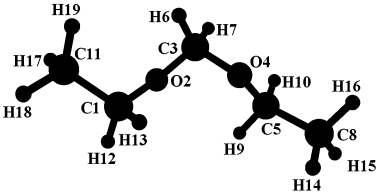

$G^{+}G^{-}(g^{+}t)$ 1.25

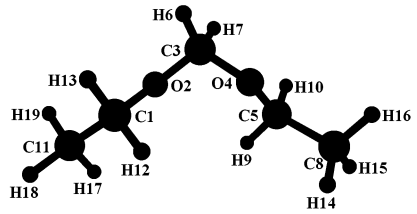

$G^{\pm}G$ (tt) 0.00

Figure 2. Structures and energies of the various conformers of DEM calculated at the B3LYP/6-31++G** level. The energy values (in kcal/mol) mentioned against each structure are relative to the **$G^{\pm}G^{\mp}$(tt)** conformer.

that the ground-state conformer in DMM had a **$G^{\pm}G^{\mp}$** structure,[16] which denotes a gauche orientation of the carbon atom attached to oxygen, the anomeric carbon atoms. For this orientation of the anomeric carbon atoms, the terminal carbon atoms in DEM can taken on various orientations. Hence, the conformers of DEM can be written as **$G^{\pm}G^{\mp}$(xy)**, where **x** and **y** stand for **t**, **g^{+}**, or **g^{-}** to denote the orientation of the terminal carbon atoms, while **$G^{\pm}G^{\mp}$** denotes the orientation of the anomeric carbon atoms. The upper case in this notation denotes the orientation of the anomeric carbon atom, while the lower case denotes that for the terminal carbon. Likewise corresponding to the conformers **$TG^{\pm}$**, **$G^{\pm}G^{\pm}$**, and **TT** of DMM, the various possible conformers of DEM can be written as **$TG^{\pm}$(xy)**, **$G^{\pm}G^{\pm}$ (xy)**, and **TT(xy)**.

At the outset, we first performed geometry optimizations at the B3LYP/6-31++G** level. At this level, we obtained six minima corresponding to a cluster of conformers that arises from the **$G^{\pm}G^{\mp}$** conformer of DMM: **$G^{\pm}G^{\mp}$(tt)**, **$G^{+}G^{-}(g^{+}t)$**, **$G^{+}G^{-}(g^{-}t)$**, **$G^{+}G^{-}(g^{+}g^{+})$**, **$G^{+}G^{-}(g^{+}g^{-})$**, and **$G^{+}G^{-}(g^{-}g^{-})$**. Similarly, nine minima were identified corresponding to a cluster of conformers that arises from the **$TG^{\pm}$** of DMM: **$TG^{\pm}$(tt)**, **$TG^{+}(g^{-}t)$**, **$TG^{+}(tg^{-})$**, **$TG^{+}(tg^{+})$**, **$TG^{+}(g^{+}t)$**, **$TG^{+}(g^{-}g^{-})$**, **$TG^{+}(g^{-}g^{+})$**, **$TG^{+}(g^{+}g^{-})$**, and **$TG^{+}(g^{+}g^{+})$**. Some selected molecular parameters that determine the structures of the various conformers are given in Table 1. The structures of the ground state and the first three higher energy conformers, which were experimentally observed, are shown in Figure 2. (Structures of all the minima have not been shown to minimize the number of figures displayed; details of the structures corresponding to all the minima can be obtained from the authors on request.)

A diagram showing the correlation between the conformers of DMM and DEM is shown in Figure 3. Also shown in Figure 3 are the energies of the various conformers of DEM (corrected for zero-point energies) relative to the lowest energy **$G^{\pm}G^{\mp}$(tt)** conformer. Alongside the energy of the conformers, the dipole moment of each of the conformers is also given in parentheses. It can be seen from Figure 3, that in the cluster of conformers of DEM correlating with the **$G^{\pm}G^{\mp}$** conformer of DMM, the lowest energy conformer corresponds to one in which the *terminal carbon atom adopts a trans orientation*, that is, **$G^{\pm}G^{\mp}$(tt)** is the lowest energy structure. Likewise, the **$TG^{\pm}$(tt)** structure of DEM is the lowest among the conformers arising from the **$TG^{\pm}$** cluster. This observation indicates that a trans disposition of the terminal carbon atom in DEM is the most favored orientation. Furthermore, the energy difference between the **$G^{\pm}G^{\mp}$** and **$TG^{\pm}$** conformers in DMM is approximately maintained between the **$G^{\pm}G^{\mp}$(tt)** and **$TG^{\pm}$(tt)** forms in DEM. This observation suggests that the **$G^{\pm}G^{\pm}$(tt)** and **TT(tt)** conformers of DEM belonging to the next higher clusters and correlating with the **$G^{\pm}G^{\pm}$** and **TT** structures of DMM must be correspondingly placed above 3.5 kcal/mol relative to the ground-state conformer. Recalling that the **$G^{\pm}G^{\pm}$** and **TT** conformers were not experimentally observed in DMM, it does not seem likely that the structures of DEM correlating with these

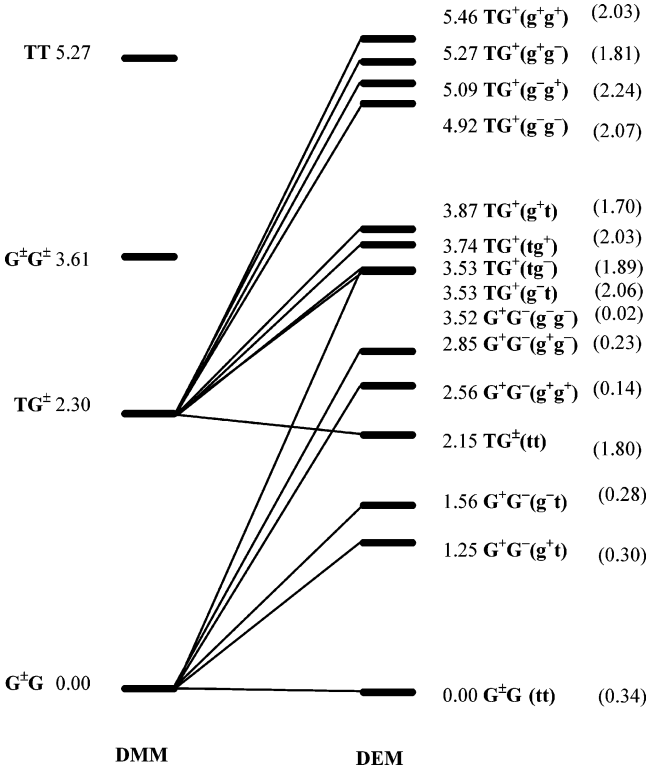

Figure 3. Diagram showing the correlation between the conformers in DMM and DEM. Energies (in kcal/mol) of each conformer relative to the ground-state conformer of the respective molecule is given. Also shown are the dipole moments (D) of the different conformers of DEM, in parentheses. All calculations were performed at the B3LYP/6-31++G** level.

structures would be observed. We therefore studied only the cluster of conformers corresponding to **G±G∓(xy)** and **TG±(xy)** structures.

Discussion

Vibrational Assignments. The main spectral features at 854.8, 1024.1, 1054.8, 1060.1, 1100.6, 1112.0, 1121.5, 1126.1, 1165.0, and 1199.9 cm^{-1}, marked in Figure 1b, are essentially those of the ground-state conformer, which is indicated from our computations to have a **G±G∓(tt)** structure. The computed frequencies at the B3LYP level, for this conformer, agree well with the spectral features obtained with a room-temperature effusive source, as can be seen from Table 2 and Figure 1, which shows the computed spectrum (Figure 1a) against the experimentally obtained spectrum (Figure 1b).

We next consider the assignment of the spectral features marked with asterisks that we believe arise from higher energy conformers. We subtracted the spectrum shown in Figure 1c (430 K nozzle) from that shown in Figure 1b (298 K nozzle), and the subtracted spectrum is shown in Figure 4d. This spectrum shows features belonging to conformers that have an increased population at 430 K. Incidentally, the features in this subtracted spectrum are those marked with asterisks in Figure 1c.

Our calculations, at the B3LYP/6-31++G** level, indicates that the first higher energy conformer with a **G+G−(g+t)** structure lies 1.25 kcal/mol above the ground state. At room temperature, the **G+G−(g+t)** form contributes to ∼10% of the total population, while at 430 K its population increases to ∼15%. Figure 4a shows the computed spectra of the **G+G−(g+t)** conformer, where the frequencies and intensities were obtained from the B3LYP computations and the simulation was done using a Lorentzian line profile and an fwhm of 1 cm^{-1}. It can be seen that the main features in the computed spectra for this conformer do appear in the experimental spectrum (Figure 4d).

TABLE 2: Comparison of Experimental and B3LYP/6-31++G Computed Vibrational Frequencies in DEM[f]**

B3LYP scaled frequencies[a] (cm^{-1})				experimental (matrix isolation)
G±G∓(tt)	**G+G−(g+t)**	**G+G−(g−t)**	**TG±(tt)**	
848.0(20)[b]				854.8 (w)[c]
	1013.4(43)	1013.4(54)	1016.3(55)	1015.5
1014.0(65)				1024.1 (s)
	1042.8(294)	1054.1(242)		1048.8, 1050.4
1060.7(253)				1054.8, 1060.1[d] (vs)
			1090.7(138)	1087.1
	1105.8(122)	1104.8(131)		1097.4
1100.6(212)			1100.8(262)	1100.6 (vs)
1114.7(15)				1112.0 (w)
1131.6(107)	1123.3(107)	1128.2(87)		1121.5,1126.1 (m)
1169.7(18)	1164.0(81)	1164.2(77)		1165.0 (w)
			1178.9(49)	1174.9
1194.9(59)			1191.0(166)	1199.9 (m)
1410.1(39)	1402.4(19)	1402.9(20)	1361.9(25)	1392.2, 1399.7[e]
1414.7(16)	1411.7(27)	1413.9(30)	1403.9(46)	
2955.0(98)	2956.0(51)	2957.5(49)	2882.0(78)	2881.1, 2887.7,
2980.5(93)	2988.0(85)	2973.6(41)	2935.2(77)	2892.5, 2909.8,
3011.3(38)	3004.9(28)	2981.7(102)	2954.0(53)	2927.2, 2936.8,
3014.9(15)	3011.3(23)	3006.4(18)	2962.0(68)	2944.6,
3016.0(37)	3019.1(25)	3011.7(22)	2998.1(65)	2986.5
3034.3(46)	3044.2(43)	3016.2(27)	3012.0(25)	2996.1
3082.2(51)	3073.0(42)	3035.8(45)	3032.1(21)	
3089.1(21)	3081.7(29)	3044.1(32)	3082.8(29)	
3089.4(46)	3088.2(43)	3072.4(35)	3084.0(30)	
	3089.1(34)	3082.1(30)	3091.0(33)	
		3089.1(34)	3092.2(29)	
		3101.7(28)		

[a] Scaling factor is 0.9890. [b] Computed intensities are in units of km/mole. [c] vs: very strong; s: strong; m: medium; w: weak. These intensity descriptors are relative and have been shown for the features of the ground-state conformers only. Features due to the higher energy conformers are weak, as the population of these conformers are small and hence no intensity descriptors are given. [d] The doublets may be due to site effects. [e] No intensity descriptors are given for these features as these could not be resolved for the different conformers. [f] The computed intensities for each mode is given in parentheses.

While the main features in the spectrum shown in Figure 4d may be assigned to the **G+G−(g+t)** conformer, minor contributions to this spectrum from other higher energy forms cannot be ruled out. The next higher energy forms, **G+G−(g−t)** and **TG±(tt)**, are located 1.56 and 2.15 kcal/mol, respectively, above the ground-state conformer. At room temperature, these two conformers would contribute ∼6% and ∼4% to the total population, while at 430 K their populations would increase to ∼10% and 8%. Hence, a contribution to the spectrum in Figure 4d from the **G+G−(g−t)** or **TG±(tt)** conformers is also possible. Because the computed vibrational spectrum of the **G+G−(g−t)** conformer (Figure 4b) very closely resembles that of the first higher energy **G+G−(g+t)** form (Figure 4a), it would be very difficult to discern the contribution of the **G+G−(g−t)** conformer, even if this conformer were present and contributing to the spectrum shown in Figure 4d. The computed vibrational spectrum of the **TG±(tt)** structure (Figure 4c) is significantly different from the first two higher energy forms. From the subtracted spectrum shown in Figure 4d, it is possible that features corresponding to the **TG±(tt)** structure are also present. Hence, the features in Figure 4d may be assigned to the **G+G−(g+t)** conformer with likely contributions from the **G+G−(g−t)** and **TG±(tt)** conformers. This study constitutes the first reported spectrum of the higher energy conformers of DEM.

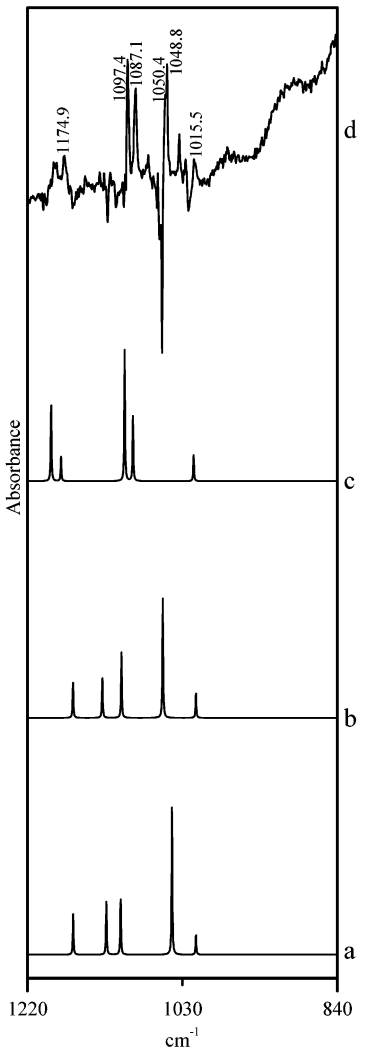

Figure 4. Computed spectra for (a) $\mathbf{G^+G^-(g^+t)}$, (b) $\mathbf{G^+G^-(g^-t)}$, and (c) $\mathbf{TG^{\pm}(tt)}$ conformers of DEM. (d) Spectrum obtained by subtracting the trace shown in Figure 1c from that shown in Figure 1b.

The vibrational assignments for these higher energy conformers are shown in Table 2.

Dipole Moments

The reported experimental dipole moment of DEM in the vapor phase is 1.23 and 1.27 D at 328−353 K and 408−473 K, respectively.[17] The computed dipole moments of the various DEM conformers using B3LYP/6-31++G** level are shown in Figure 3. Using the computed dipole moments at the B3LYP level for each conformers, $\mathbf{G^{\pm}G^{\mp}(tt)}$, $\mathbf{G^+G^-(g^+t)}$, $\mathbf{G^+G^-(g^-t)}$, and $\mathbf{TG^{\pm}(tt)}$, the dipole moment of DEM averaged over the different conformers was calculated. The dipole moments were calculated for 353 and 473 K, which are the temperatures for which experimental values have been reported. The dipole moments of DEM thus calculated were 0.57 and 0.70 D, at 353 and 473 K respectively, which is however lower than the respective experimental values of 1.23 and 1.27 D.

Comparison of the Conformational Picture in DMM and DEM

The substitution of a methyl group for one of the hydrogens on the terminal carbon atoms of DMM introduces additional rotational degrees of freedom, that is, C−C−O−C in DEM compared with the C−O−C−O and O−C−O−C rotations in DMM. A diagram (Figure 3) can therefore be drawn to correlate the conformations of the two molecules. It can be seen from Figure 3 that the $\mathbf{G^{\pm}G^{\mp}}$ and $\mathbf{G^{\pm}G^{\mp}(tt)}$ conformers are the ground states in DMM and DEM, respectively. The stability around the O−C−O bond is decided by the two anomeric interactions involving the nonbonded electrons of both the oxygens. The stability around the C−C−O bond is decided by steric interactions, which is equivalent of the stability pattern in alkanes. As the terminal carbon atoms in the ground-state conformer of DEM are progressively converted to gauche orientations, the energy rises, for example, the energy of the $\mathbf{G^+G^-(g^+t)}$ form is 1.25 kcal above the ground state. At the B3LYP/6-31++G** level, the energy difference between the $\mathbf{G^{\pm}G^{\mp}}$ and $\mathbf{TG^{\pm}}$ conformers in DMM (2.30 kcal/mol) is approximately maintained between the $\mathbf{G^{\pm}G(tt)}$ and $\mathbf{TG^{\pm}(tt)}$ conformers in DEM (2.15 kcal/mol).

We also examined the possibility of any intramolecular hydrogen-bonding interactions being involved in stabilizing any of these conformers. An examination of the charge density topology using the atoms-in-molecule (AIM) theory of Bader[18] showed that (3, −1) bond critical points that could be associated with intramolecular C−H···O interactions could be identified only in the $\mathbf{G^+G^-(g^-t)}$, $\mathbf{G^+G^-(g^+g^-)}$, $\mathbf{G^+G^-(g^-g^-)}$, $\mathbf{TG^+(tg^-)}$, $\mathbf{TG^+(g^-g^-)}$, and $\mathbf{TG^+(g^+g^-)}$ conformers. However, these conformers do not contribute significantly at room temperatures, and therefore it must be concluded that at least for the ground state and lower energy conformers that populate room temperature samples, only anomeric and steric effects are the major contributing factors for conformer stability in DEM.

Conclusions

We have recorded for the first time the infrared spectra of matrix-isolated DEM, in an argon matrix. Spectral features of the ground state $\mathbf{G^{\pm}G^{\mp}(tt)}$ and the excited $\mathbf{G^+G^-(g^+t)}$, $\mathbf{G^+G^-(g^-t)}$, $\mathbf{TG^{\pm}(tt)}$ conformers were observed. The experimental vibrational frequencies of the above conformers agreed well with the values calculated at the B3LYP/6-31++G** level. This work has led to definitive assignment of the various infrared features of DEM.

Even though not experimentally observed, we also located minima correlating with the other excited state conformers corresponding to the $\mathbf{G^{\pm}G^{\mp}}$ and $\mathbf{TG^{\pm}}$ clusters.

From this study, it is clear that in DEM the carbon atom attached to oxygen adopts a gauche orientation, while the terminal carbon atoms in the alkyl groups prefer a trans orientation, mimicking the behavior in alkanes. The above conclusion is useful as it allows for an understanding of the conformers of long-chain acetals and ketals, and also long-chain organic phosphates, which will be the subject of future studies.

Acknowledgment. V.V. gratefully acknowledges the grant of a research fellowship from the Department of Atomic Energy, India.

References and Notes

(1) Thatcher, G. R. J. *The Anomeric Effect and Associated Stereoelectronic Effects*; ACS Symposium Series 539; American Chemical Society: Washington, DC, 1993.

(2) Juaristi, E.; Cuevas, G. *The Anomeric Effect*; CRC Press: Boca Raton, FL, 1995.

(3) Andrews, C. W.; Bowen, J. P.; Fraser-Reid, B. J. *J. Chem. Soc. Chem. Commun.* **1989**, 1913.

(4) Ganguly, B.; Fuchs, B. *J. Org. Chem.* **1997**, *62*, 8892.

(5) Venkatesan, V.; Sundararajan, K.; Sankaran, K.; Viswanathan, K. S. *Spectrochim. Acta* **2002**, *58A*, 467.

(6) Venkatesan, V.; Sundararajan, K.; Viswanathan, K. S. *J. Phys. Chem. A* **2002**, *106*, 7707.

(7) Venkatesan, V.; Sundararajan, K.; Viswanathan, K. S. *Spectrochim. Acta A* **2003**, *59*, 1497.

(8) Nukada, K. *Spectrochim. Acta* **1961**, *34*, 1615.

(9) Nukada, K. *Spectrochim. Acta* **1961**, *34*, 1624

(10) George, L.; Sankaran, K.; Viswanathan, K. S.; Mathews, C. K. *Appl. Spectrosc*. **1994**, *48*, 7.

(11) Vidya, V.; Sankaran, K.; Viswanathan, K. S. *Chem. Phys. Lett*. **1996**, *258*, 113.

(12) George, L.; Viswanathan, K. S.; Singh, S. *J. Phys. Chem. A* **1997**, *101*, 2459.

(13) Frisch, M. J.; Trucks, G. W.; Schlegel, H. B.; Gill, P. M. W.; Johnson, B. G.; Robb, M. A.; Cheeseman, J. R.; Keith, T.; Petersson, G. A.; Montgomery, J. A.; Raghavachari, K.; Al-Laham, M. A.; Zakrzewski, V. G.; Ortiz, J. V.; Foresman, J. B.; Peng, C. Y.; Ayala, P. Y.; Chen, W.; Wong, M. W.; Andres, J. L.; Replogle, E. S.; Gomperts, R.; Martin, R. L.; Fox, D. J.; Binkley, J. S.; Defrees, D. J.; Baker, J.;. Stewart, J. J. P.; Head-Gordon, M.; Gonzalez, C.; Pople, J. A. *Gaussian 94*, Revision E.1; Gaussian, Inc.: Pittsburgh, PA, 1995.

(14) The spectra were simulated using the program, SYNSPEC, made available by Irikura, K. National Institute of Standards and Technology: Gaithersburg, MD, 20899, 1995.

(15) Dasgupta, S.; Smith, K. A.; Goddard, W. A., III *J. Phys. Chem*. **1993**, *97*, 10891.

(16) For a discussion on the notation used to denote the conformers of the DMM moiety, see ref 6 in this paper.

(17) McClellan, A. L. Tables of experimental dipole moments; W. H. Freeman and Co: San Francisco, CA, 1963; Vol. 1.

(18) Bader, R. F. W. *Atoms in Molecules*; Clarendon Press: Oxford, U.K., 1994.